^{15}N Chemical Shifts and Long-Range ^{1}H-^{15}N Coupling Pathways of Selected *Strychnos* Alkaloids

Gary E. Martin* and Ronald C. Crouch

Bioanalytical Sciences, Burroughs Wellcome Co., Research Triangle Park, NC 27709

C. Webster Andrews

Division of Organic Chemistry, Burroughs Wellcome Co., Research Triangle Park, NC 27709

Received August 11, 1995

The *Strychnos* alkaloids have been the focal point of considerable synthetic and spectroscopic effort. We now report the ^{15}N chemical shifts and long-range ^{1}H-^{15}N coupling pathways of strychnine, brucine, and holstiine at natural abundance. Long-range coupling pathways were established using a gradient-enhanced HMQC sequence optimized for the observation of ^{1}H-^{15}N long-range couplings.

J. Heterocyclic Chem., **32**, 1759 (1995).

Introduction.

We recently reported a method for long-range ^{1}H-^{15}N heteronuclear shift correlation [1], demonstrating the technique with the model alkaloid ajmaline. We now wish to report the extension of our previous efforts to several members of the *Strychnos* family of alkaloids, including strychnine (**1**), brucine (**2**), and holstiine (**3**).

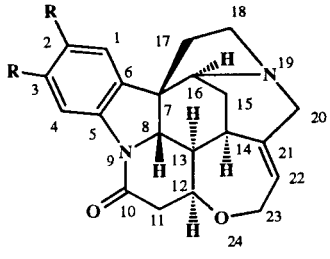

1 R = -H

2 R = -OCH_3

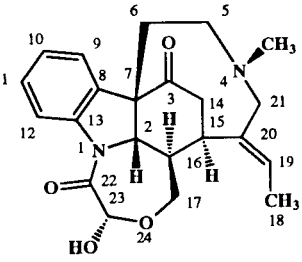

3

Resonance assignments for strychnine [2-5], brucine [6], holstiine [7] have been reported, and were confirmed using the recently reported IDR-GHMQC-TOCSY [8] experiment or a combination of GCOSY [9] and pure phase-sensitive GHMQC spectra [10-12] as necessary. Proton stereochemical orientations were reconfirmed from phase-sensitive NOESY spectra.

^{1}H-^{15}N Spectroscopy of Strychnine.

Unequivocal ^{1}H resonance assignments for strychnine in deuterochloroform were confirmed on the basis of IDR-GHMQC-TOCSY spectra acquired with mixing times of 18 and 30 msec. The reassignment process precluded any possibility of an exchange of the resonance positions of the partially overlapped H18a, H14, and H11α resonances near 3.1 ppm as a function of concentration.

A series of three long-range ^{1}H-^{15}N gradient-enhanced heteronuclear shift correlation spectra of strychnine (**1**) were acquired overnight optimized for 5, 8, and 10 Hz. The F_1 spectral window was set from 20-170 ppm (chemical shifts are reported in ppm downfield of liquid ammonia which was taken as 0 ppm). As expected, two sets of responses were observed in the spectra of the 10 Hz optimized spectrum shown in Figure 1. The aliphatic N19 resonance was correlated to numerous proton resonances and was observed upfield at 35 ppm. In contrast, the amide N9 resonance was observed downfield at 148 ppm as expected.

Four of the six long-range couplings to N19 observed in the contour plot were via two-bonds ($^{2}J_{NH}$) and included: H16-N19, H20α-N19, H18α-N19, and H18β-N19. Of these correlations, the H16-N19 correlation was most intense (see Figure 2) while that from H18β-N19 was the weakest visible in the contour plot. From the slice taken at 35 ppm shown in Figure 2 plotted above a ^{1}H reference spectrum, there is a very weak response that may be attributable to a weak $^{2}J_{NH}$ correlation from H20β-N19 that was below the threshold used to prepare the contour plot. The remaining long-range couplings observed were three-bond ($^{3}J_{NH}$) correlations from either H17α or H17β-N19 and from H15α-N19. In the case of the former proton resonances, which are strongly overlapped even at 500 MHz, a definitive assignment of the coupling pathway could not be established on the basis of the available spectral data.

Examination of a minimized molecular model of strychnine (**1**) was particularly informative in regard to the observed two-bond couplings to N19. The minimized structure of strychnine is shown, **4** (the two molecular models of strychnine derived from a Monte Carlo search for structures are shown in Figure 3), viewed looking toward the aliphatic N19 approximately along the axis of the lone pair, i.e. from the "back". As will be noted from this vantage-point, the H16 resonance, H18α, and the H20α resonances are oriented more or less synclinally with the nitrogen lone pair. The remaining H18β and H20β resonances are more anticlinally oriented. Based on previous work [2,13-17], protons capable of engaging in two-bond couplings which are oriented synclinally to the nitrogen lone pair are expected to exhibit much larger $^{2}J_{NH}$ couplings. In the two-

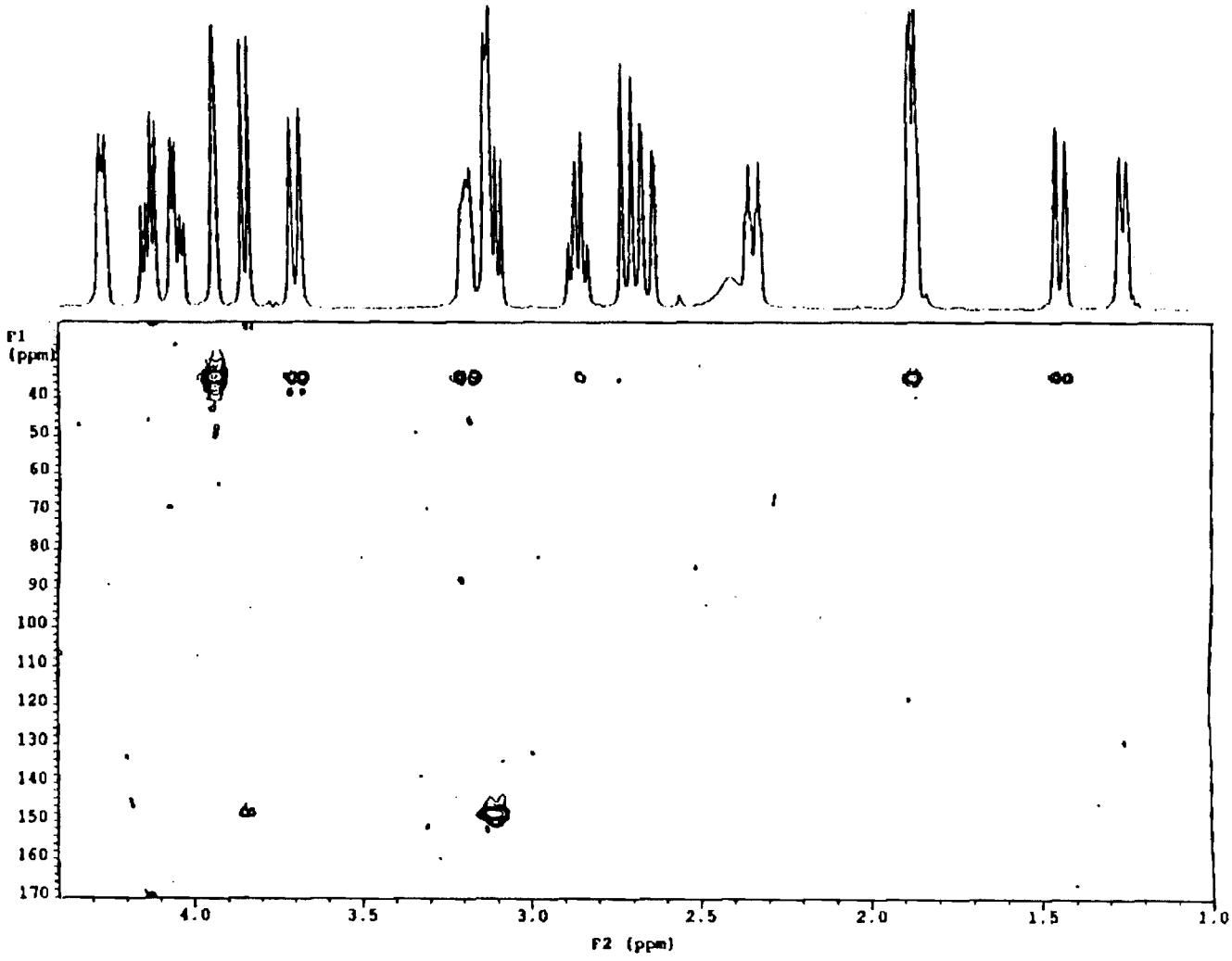

Figure 1. Long-range ^{1}H-^{15}N heteronuclear shift correlation spectrum optimized for 10 Hz acquired using a sample consisting of 0.045 mole of strychnine (**1**) dissolved in 0.65 ml of 99.96% d_6-DMSO. The data were acquired as 4736 x (96 x 2) hypercomplex files with a total of 96 transients accumulated/file giving a total acquisition time of 12 hours. A high resolution proton reference spectrum is plotted atop the contour plot.

dimensional experiment, we consequently would anticipate that a larger heteronuclear coupling, based on optimization considerations, would equate to a more intense response. Long-range couplings that could be measured (see **4**) were consistent with this expectation.

Three-bond proton-nitrogen correlations to N19 were possible from protons at the 15- and 17-positions. In the case of the former, the $^{3}J_{NH}$ dihedral angles for 15α and 15β were -168.6° and -47.9°, respectively, as shown by **4**. Karplus relationships governing $^{3}J_{NH}$ coupling pathways have been shown [14] to have maxima near 0° and 180° with a minimum in the vicinity of 90°. Thus, the $^{3}J_{H15\alpha N19}$ coupling of 7 Hz is reasonable given the dihedral angle between H15α-N19. It is equally reasonable that no correlation was observed between H15β-N19 in view of the dihedral angle between these nuclides, which would be expected to lead to a small three-bond coupling.

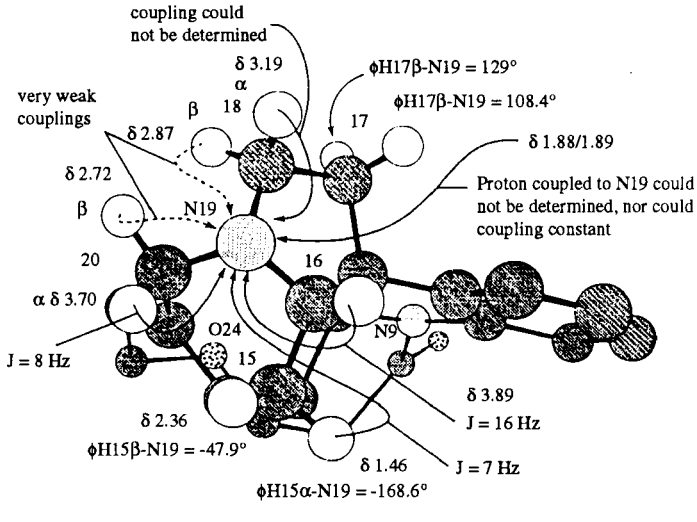

4

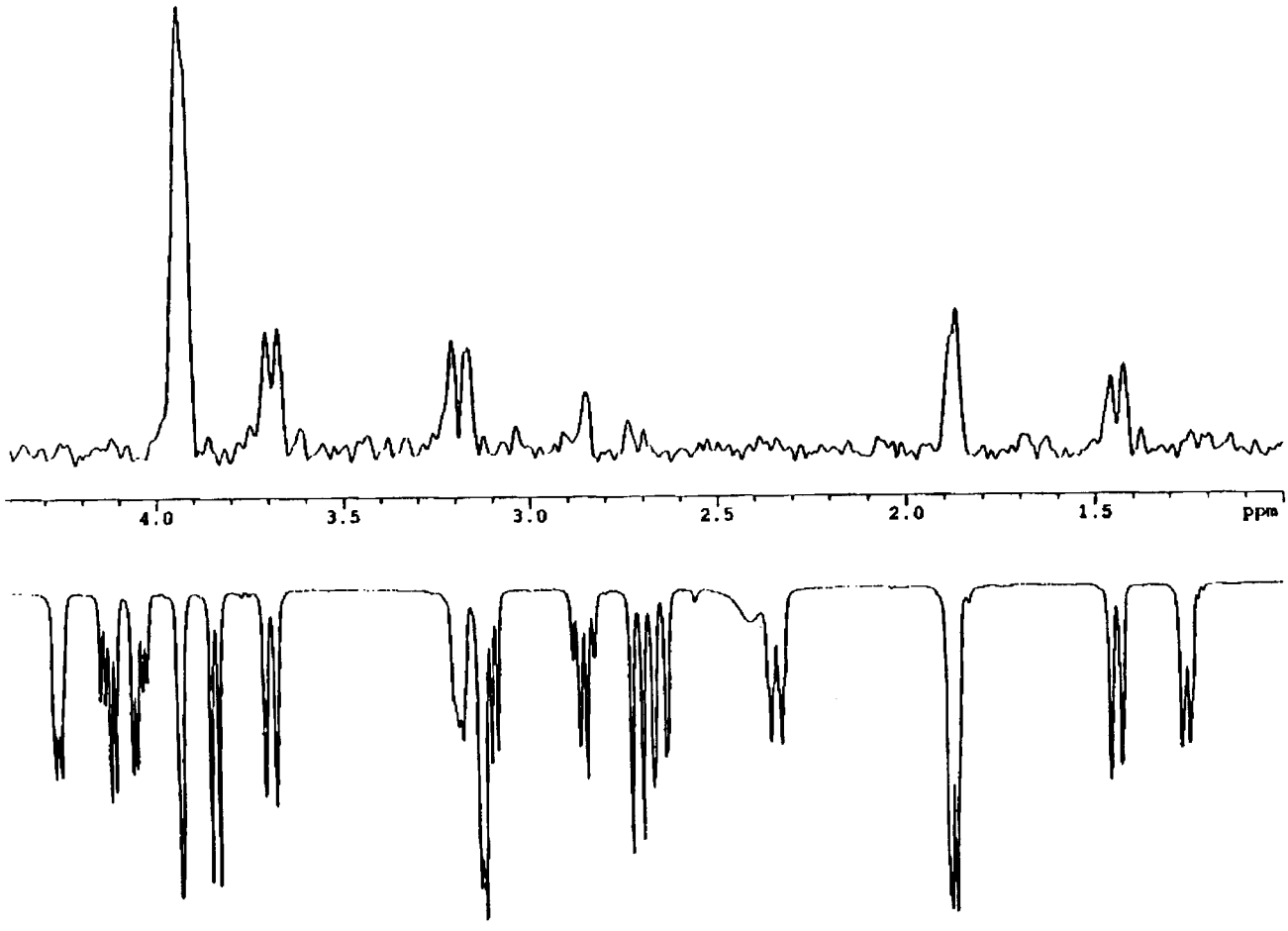

Figure 2. Top trace taken at 34.9 ppm from the 10 Hz optimized long-range ^{1}H-^{15}N heteronuclear shift correlation spectrum of strychnine (**1**) shown in Figure 1 containing long-range correlations to the aliphatic N19 resonance. An inverted phase proton reference spectrum is plotted beneath the trace from the 2D data matrix. The s/n ratio in the trace shown was 44:1 for a 12 hour acquisition. For comparison, the s/n for the corresponding trace in the 8 Hz optimized spectrum with an acquisition time of 4.5 hours was 14:1. Responses in the trace from the 2D spectrum were all observed in the contour plot shown in Figure 1 with the exception of the very weak response at ~2.72 ppm which presumably arises from a long-range coupling to the anticlinially oriented H20β resonance.

Correlations to the amide N9 resonance were more sparse than those to N19. Only a weak two-bond coupling between H8-N9 and a much more intense three-bond correlation from H11α-N9 were observed. There was no trace of three-bond correlations from either the aromatic H4 resonance or the aliphatic H13 resonance to N9. Of the three-bond coupling possibilities to N9, the correlation from H11α is reasonable given the N9-H11α dihedral angle of ϕ = -178.8°, which corresponds to one of the maxima of the Karplus curve. Of the two remaining three-bond coupling possibilities to N9, we were not surprised that no correlation was observed from H4 despite the favorable dihedral angle of ϕ = 0°. Our experience with $^{3}J_{NH}$ correlations in aromatic systems has shown these couplings to be quite weak and difficult to observe unless the experiment is optimized for very small couplings (*e.g.* 4 Hz or less [1,18,20]). Likewise, the dihedral angle between H13-N9 ϕ = 61.9°, was comparable to that between H15βN19 of ϕ = -47.9°, which exhibited no long-range coupling to N19. Both of the dihedral angles, H13-N9 and H15βN19, are approaching the minimum of the Karplus relationship which is presumed to be at or near 90°.

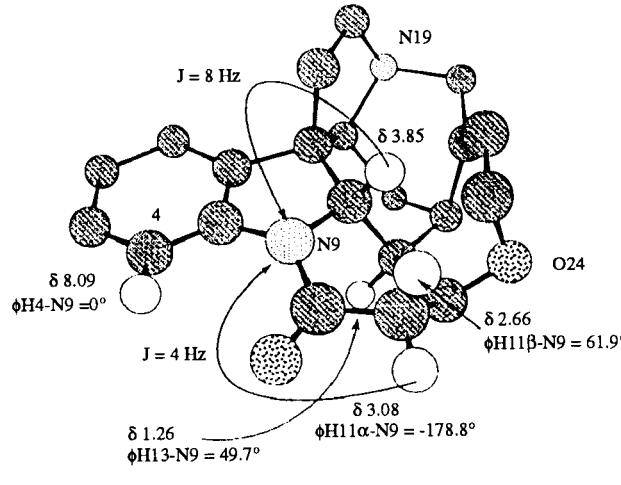

^1H-^{15}N Spectroscopy of Brucine.

Proton resonance assignments for brucine (**2**) in deuteriochloroform reported by Bernstein and Hall [6] were confirmed in d_6-DMSO using a combination of GCOSY [9], GHMQC [12], and IDR-GHMQC-TOCSY [8] spectra. Stereochemical orientation of critical proton resonances were confirmed from a NOESY spectrum recorded with a mixing time of 200 msec.

A series of long-range ^1H-^{15}N gradient enhanced heteronuclear shift correlation spectra optimized for 3, 5, 8, and 10 Hz were acquired overnight. Acquisition times for the 3, 5, and 8 Hz spectra were 4.5 hours; the acquisition time for the 10 Hz spectrum was 9 hours. The F_1 spectral window was optimized for 20-170 ppm as used with strychnine. Again, two sets of long-range couplings to ^{15}N were observed. The aliphatic N19 resonated at 37 ppm; the amide N9 resonance was shifted slightly downfield relative to strychnine, resonating at 151 ppm.

Seven long-range couplings were observed to N19 paralleling those observed for strychnine as shown by **6**. Two-bond correlations included couplings from H16, H18α, H18β, H20α, and H20β. Three-bond couplings were observed from one of the H17 resonances and H15α. Of these correlations, those from H18β and H20β were relatively weak compared to the others. The specific H17 resonance long-range coupled to N19 could not be determined because of spectral overlap of this strong AB system at 500 MHz.

Specific coupling constants observed for the long-range couplings to N19 in brucine paralleled those observed for strychnine. The synclinally oriented H16, H18α, and H20α protons all exhibited relatively large couplings to N19 of 15, 8.5, and 5 Hz, respectively. In contrast, the anticlinally oriented H20β proton was weakly coupled to N19, as was the H18β resonance. The coupling of the former to N19 could not be reliably measured although that from the latter could and was 2 Hz. The three-bond coupling from H15α to N19 was 7 Hz, identical to the corresponding coupling observed for strychnine. Because of the strong AB character of the H17 resonances, neither the coupling nor the coupling constant could be measured reliably although, based on the intensity of the response, it is reasonable to conclude that the coupling constant is relatively large.

A total of four long-range couplings were observed to the N9 resonance of brucine as shown by **7**, in contrast to only two in the case of strychnine. A 4 Hz two-bond coupling was observed from H8-N9. There were three three-bond couplings observed to N9. The strongest of these responses was a 4 Hz coupling from the H11α resonance. A moderate intensity long-range coupling was observed to H13 and a weak correlation was observed to the aromatic H4 resonance. The H13-N9 coupling constant could not be determined because of the relative complexity of the H13 multiplet. The H4-N9 coupling was a scant

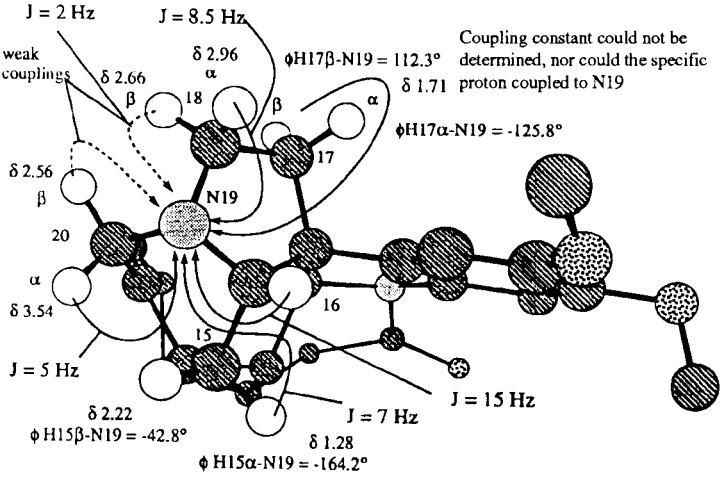

6

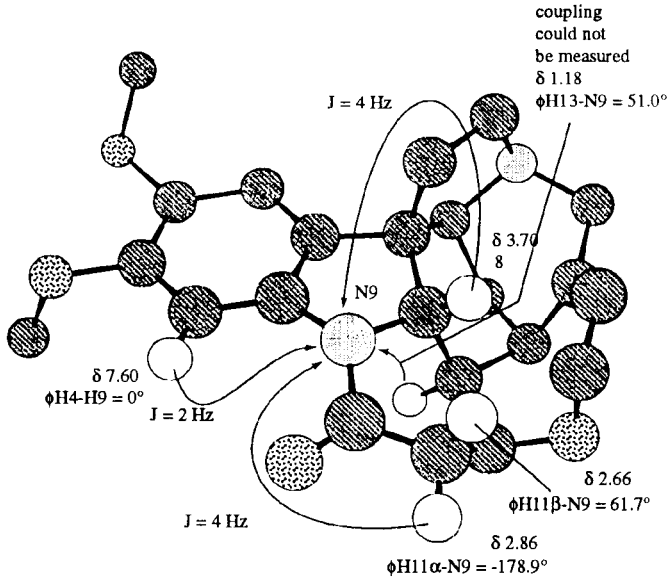

7

2 Hz. While the $^3J_{N9H4}$ coupling was observable though weak in the 8 Hz optimized spectrum, it was more pronounced in the 4 Hz optimized spectrum. Counter-productively, though, a number of the long-range couplings to N19 were either lost or observed with substantially attenuated response intensity in the 4 Hz optimized spectrum. This observation strongly suggests that optimization for particularly small couplings (*e.g.* 3-5 Hz perhaps) should be reserved for those cases when another experiment has been performed optimized for a larger long-range coupling (*e.g.* 8-12 Hz) or when dealing with a planar aromatic alkaloid such as those from *Cryptolepus sanguinolenta* [18,20,23].

^{1}H-^{15}N Spectroscopy of Holstiine.

The alkaloid holstiine (**3**) differs somewhat from strychnine and brucine in terms of its basic ring skeleton. Indeed, the structure of holstiine was not unequivocally established until 1990 [7]. In particular, the carbon-carbon bond between what would be the 16-position of strychnine and the aliphatic N19 is opened. The δ-lactam containing the N9 resonance of strychnine is expanded to an oxazepinone in the structure of holstiine, with the oxepin ring of strychnine opened and missing. Given these structural changes, there would obviously be differences in the long-range ^{1}H-^{15}N coupling possibilities of holstiine although there would probably not be major changes in the chemical shifts of the two nitrogens, making holstiine an interesting candidate for study via long-range ^{1}H-^{15}N heteronuclear shift correlation. At this point, it should also be noted that the differences in the skeleton of holstiine relative to strychnine and brucine have led to a numbering scheme for the former which differs somewhat from the latter two compounds. The numbering scheme for holstiine is shown above and will be used to describe long-range couplings of this alkaloid. Any reference to corresponding couplings from protons in strychnine and brucine will be specified parenthetically.

As expected, the long-range ^{1}H-^{15}N spectra of holstiine (**3**), optimized for 5, 8, and 10 Hz, showed two sets of responses to nitrogens resonating at 39.5 and 146.5 ppm. Clearly, based on the ^{15}N chemical shift behavior of strychnine and brucine discussed above, the nitrogen resonating upfield may be assigned as the N-methylated aliphatic N4 resonance; the downfield ^{15}N resonance is assignable as the oxazepinone N1 resonance. Correlations to the two nitrogens in the long-range ^{1}H-^{15}N spectra of holstiine (see correlations illustrated with structure **8**) were considerably more sparse than in the spectra of strychnine (**1**) and brucine (**2**). While it is attractive to speculatively attribute the paucity of responses to the greater flexibility inherent to the molecule in the azanonine ring containing N4 (due to the absence of the bond that would connect N4-C3 (N19-C16 for strychnine/brucine)), it is not feasible to experimentally confirm this supposition. It is worth noting, however, that we have recently demonstrated [19] from a Monte Carlo molecular modeling search that the azanonine ring contained in velbanamine portion of 3,4-anhydrovinblastine has three preferred families of conformations, which may parallel the behavior in the case of holstiine. Furthermore, when the structure of holstiine was modeled using Chem3D, there were two conformations apparently associated with minima for the azanonine ring. One conformation oriented the *N*-methyl in the general direction of the 3-carbonyl (equivalent location of 16-position of strychnine/brucine) moiety; the other had the *N*-methyl oriented in the general direction of the 22-cabonyl moiety (the latter representation is shown by **7**). These results suggested that more extensive molecular modeling would be appropriate to probe the issue of the conformational mobility of the azanonine portion of the molecule. It should also be noted that the responses observed in the long-range ^{1}H-^{15}N spectra of holstiine were also more sensitive to the optimization of the experiment, particularly in the case of the lone response correlating the H16α resonance to N1 *via* $^{3}J_{NH}$, which was observed with appreciable intensity only in the 5 Hz optimized spectrum.

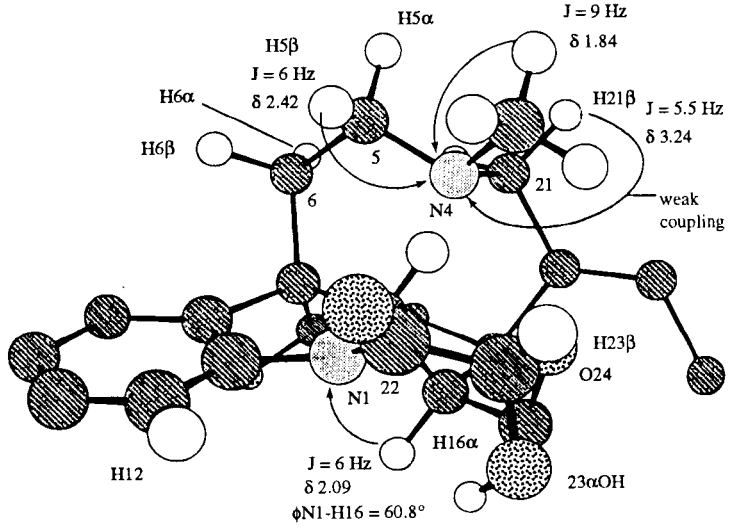

8

Another interesting feature of the correlations to N4 in the azanonine ring is the distinct absence of three-bond correlations to either of the H6 resonances. In contrast, correlation to at least one of the corresponding H17 resonances was prominent in the long-range ^{1}H-^{15}N spectra of both strychnine and brucine. Once again, it is attractive to attribute this behavior to the flexibility of the azanonine ring.

Long-range couplings to N1 also differ from those observed to the corresponding N9 resonance of strychnine and brucine. For example, the long-range ^{1}H-^{15}N spectra of both strychnine and brucine exhibited intense three-bond couplings to the H11α resonance, which was oriented at a dihedral angle of ϕ ~179° to N9 in both molecules. In the case of holstiine, although the H23β resonance is oriented favorably at a dihedral angle of ϕ = 162° relative to N1, there is no trace of a correlation to N1. Likewise, the prominent two-bond correlation from H8-N9 in the spectra of both strychnine and brucine has no corresponding two-bond H2-N1 coupling in the case of holstiine (**3**). Finally, there is also no sign of a correlation from H12-N1 although the absence of this coupling should not be considered noteworthy since these couplings, in our experience, are frequently absent in planar aromatic alkaloids [1,18,20].

Molecular Modeling.

Structures of strychnine (**1**) and holstiine (**3**) were built in MacroModel 4.5 [21] and minimized with the MM3* force field in MacroModel which is derived from the MM3 force field [22]. They were then subjected to Monte Carlo global conformational searching using the default MCMM (Monte Carlo Multiple Minimum) setup in MacroModel. MacroModel automatically defines chiral centers for constraint, identifies rotable bonds for Monte Carlo scanning, selects the number of rotable bonds which are varied during a Monte Carlo step, minimizes each Monte Carlo candidate, manages the population of low energy conformations within a 50 kJ window, and selects a starting conformation for the next Monte Carlo step from this population on the basis of least usage. The Truncated Newton (TNCG) minimization method was chosen to achieve good convergence in minimization.

Conformational analysis of strychnine (**1**) and holstiine (**3**) was initiated to compare the flexibility of their related ring systems. 2000 Monte Carlo structures were generated for holstiine, the more flexible of the two molecules, while 500 Monte Carlo structures were generated for strychnine. The results indicated that this was sufficient sampling since each output structure was generated multiple times. The conformations resulting from each search were minimized to ensure that the RMS gradients were acceptably low.

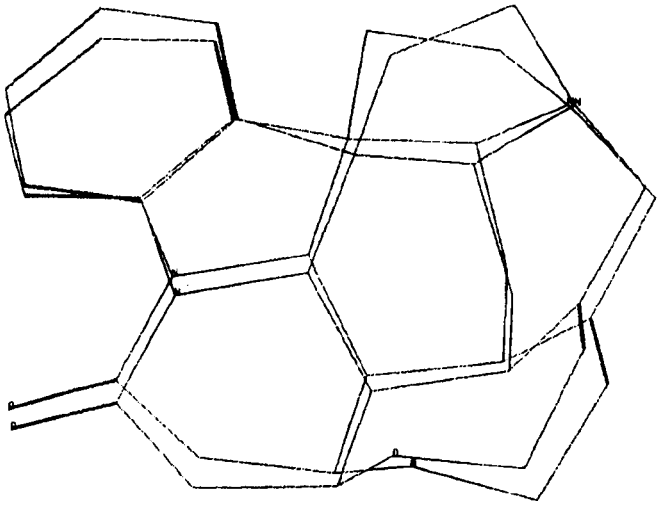

Figure 3. Superimposed structures of strychnine (**1**) within a 50 kJ window found in a Monte Carlo search for 500 structures. The structures shown had an energy spacing of 15.8 kJ (3.8 kcal) and were conformationally quite similar.

Only two conformations within the 50 kJ energy window were found for strychnine (**1**), with an energy spacing of 15.8 kJ (3.8 kcal). These conformations were superimposed and were quite similar as shown in Figure 3 (C-H hydrogens are not shown). In contrast, holstiine (**3**) yielded 33 conformations within the 50 kJ window. Six of these were within 12 kJ (about 3 kcal) of the global minimum. These six structures were superimposed and are shown in Figure 4. There are, as expected from the nmr work and the preliminary modeling cited above, two regions of flexibility in the molecule. One region of flexibility, as expected, was in the azanonine ring. The other region of high flexibility was in the seven-membered oxazepinone ring.

It is interesting to speculate on the consequences of the conformational flexibility of holstiine (**3**) on the correlations observed in the long-range ^{1}H-^{15}N heteronuclear shift correlation experiments. First, for the relatively strong correlation observed from H5β to N4 (J = 6 Hz) to be feasible, the H5β resonance must be oriented synclinally to the lone pair of N4. Examining the six lowest energy conformations of holstiine shown in Figure 4, three of the six (the two lowest and sixth conformers)

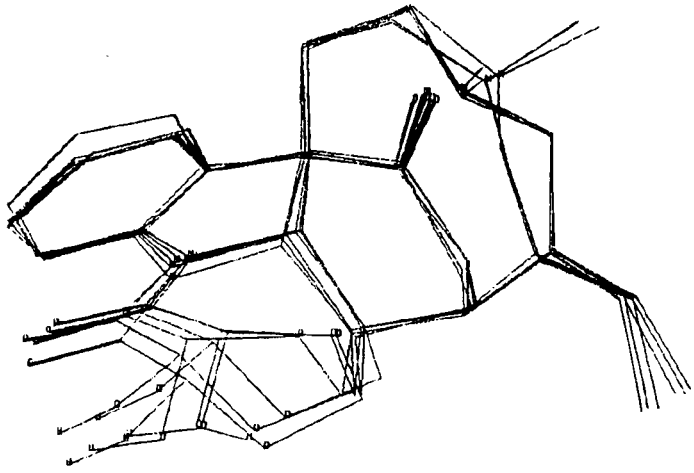

Figure 4. Six superimposed structures of holstiine (**3**) of 33 structures found within a 50 kJ window found in a Monte Carlo search for 2000 structures. The structures shown had an energy spacing of about 12 kJ (~3 kcal). Within the azanonine ring, there were two preferred families of orientations, each containing three structures. One family had the N4-Me pointed toward the back of the molecule, generally in the direction of the 1 6-carbonyl moiety. The other conformational family had the N4-Me pointed forward. The latter group contained the two lowest energy conformers which differed from one another by about 6 kJ. The three conformational members of the former family (N4Me back) ranged from 4-6 kJ higher in energy as did the remaining member of the latter family (N4-Me forward). There is also a region of considerably conformation flexibility in the models of holstiine (**3**) in the region of the oxazepinone ring containing N1. The most flexible region involves the 23- and 24-positions and may account for the lack of a correlation between the H23β proton and N1, which would be in a position analogous to that of the H11 a proton of strychnine (**1**) and brucine (**2**), which exhibited strong couplings to N9 in the case of both 1 and 2.

would bring H5β into a reasonable orientation relative to the lone pair to account for the strong response observed. In contrast, the H21β resonance, which has a 5.5 Hz coupling to N4, exhibits a much weaker response correlating

it to N4. This observation suggests that while H21β has a synclinal orientation relative to the N4 lone pair, it spends a greater percentage of time, on the nmr time scale, at least, with an orientation which is anticlinal a greater percentage of time than it is synclinally oriented.

Molecular modeling also provides interesting insights into the long-range couplings to the N1 amide resonance in the oxazepinone ring; there is a distinct absence of any long-range correlation from the H23β proton to N1. Despite the fact that the H23β resonance is oriented favorably to allow a three-bond coupling analogous to that of H11α in the case of strychnine (**1**) and brucine (**2**), the coupling is still not observed. From a modeling perspective, however, this would appear to be reasonable since there is a greater degree of conformational mobility associated with the 22- and 23-positions of the oxazepinone ring than even that involving N4. Furthermore, since some of the six lowest energy conformations would position the H23β proton such that it would be oriented with a dihedral angle of near 90° relative to N1 which, being near the minimum of the Karplus curve, could easily account for the lack of resopnse from H23β to N1.

Hence, from the broad perspective, the molecular modeling results are congruent with the results of the long-range ^{1}H-^{15}N heteronuclear shift correlation experiments performed on holstiine and strychnine.

Conclusions.

In conclusion, we have shown that long-range ^{1}H-^{15}N coupling pathways can be studied in complex alkaloids at natural abundance with reasonable facility by using a gradient-enhanced variant of the HMQC pulse sequence. For the trio of *Strychnos* alkaloids comprised of strychnine (**1**), brucine (**2**), and holstiine (**3**), the ^{15}N chemical shift of the two nitrogens exhibited considerable regularity, as shown in Table 1. Coupling pathways observed for the strychnine and brucine, which are structurally identical except for the 2,3-dimethoxyl substitution of the latter, were comparable, leading to the possibility of exploiting long-range ^{1}H-^{15}N couplings as a structural probe in just a few hours when sufficient quantities, *e.g.* 0.02-0.04 mmoles, are available for study. Long-range ^{1}H-^{15}N correlation experiments could also be performed on smaller quantities of material by resorting to either overnight data acquisition and/or micro inverse-detection. We have demonstrated the usage of the latter for one-bond non-gradient ^{1}H-^{15}N heteronuclear shift correlation overnight on a sample of 3.4 μmoles of the simple alkaloid quindolinone [23]. While the long-range experiment probably cannot be performed with this efficiency, it would be possible to study samples of 0.01 mmole or less overnight when gradient micro inverse-detection is utilized. We have shown that two-bond couplings tend to be the most intense when the proton coupling to ^{15}N is oriented synclinally to the nitrogen lone pair of electrons; when two-bond couplings were observed for protons oriented anticlinally, they were uniformly weaker than for a synclinally oriented proton. Finally, the NMR observations reported in this study, in conjunction with the molecular modeling results, suggest the possibility of molecular motion in the azanonine and oxazepinone rings of holstiine (**3**) influencing the observation of three-bond couplings between the protons in that ring and their respective ^{15}N resonances, a factor which requires further evaluation.

Table 1

Summary of ^{15}N Chemical Shifts of Strychnine, Brucine, and Holstiine Determined from Long-Range ^{1}H-^{15}N Heteronuclear Shift Correlation Data

	δ^{15}N N9 (N1) [a]	δ^{15}N N19 (N4) [a]
Strychnine	148.0	35.0
Brucine	151.0	37.0
Holstiine	146.5	39.5

[a] Positional labels for holstiine (**3**) are shown in parentheses. ^{15}N Chemical shifts are reported downfield from liquid ammonia and are assumed to be accurate to ±0.5 ppm and have been rounded to the nearest 0.5 ppm. Chemical shifts can be rereferenced to neat nitromethane which resonates 379.5 ppm downfield of liquid ammonia by subtracting the chemical shift given in the table from that of neat nitromethane. The sign convention relative to neat nitromethane is reversed, hence all of the nitrogen chemical shifts reported in this study would be upfield and positive relative to nitromethane.

EXPERIMENTAL

All of the experiments described in this paper were performed using a three channel Varian Unity 500 spectrometer equipped with Performa II PFG hardware and a Nalorac Z•SPEC® IDTG-500-5 triple resonance probe. The pulse sequence used was that contained in our previous report [1]; the code employed for the gradient-enhanced ^{1}H-^{15}N heteronuclear shift correlation utilized channels 1 and 3. Measured pulse widths for ^{1}H and ^{15}N ranged from 9.6-9.8 μsec for ^{1}H and 30.0 μsec for ^{15}N at power settings of 56 and 63 dB, respectively (63 dB maximum). A maximum gradient strength of ~40 Gcm^{-1} (0.040 T) was possible with the combination of hardware used for these studies. Gradient pairs of 5:5:1 and 5:5:-1 were used and the data were acquired in a fully phase-sensitive fashion. Tweaked DAC values corresponding to the gradient ratios used were 10000, 10000, and ±2010. The duration of all gradients was 1.5 msec. Although the data were acquired in a fully phase-sensitive fashion to expedite the extraction of long-range ^{1}H-^{15}N coupling constants whenever possible, the data could not be presented in a fully phase-sensitive manner since the duration of the gradient times was not compensated for by 180° refocusing pulses. Instead, ^{15}N resonances were individually phased in F_1, transposed and the ^{1}H-^{15}N coupling extracted from phased F_2 slices. The data were uniformly acquired as 4096 x (128 x 2) hypercomplex files and were zero-filled to 8192 x 512 during processing. All experiments were acquired with a uniform F_1 spectral

window of 20-170 ppm for ^{15}N. Experiments were variously optimized for long-range couplings of 5, 8, 10, or 12 Hz as described in the text. Typical acquisition times ranged from 4.5 to 9 hours depending on the number of transients accumulated/t_1 increment (64-128 transients). Usable data could be obtained for all but the weakest of responses in one-half to one-quarter of the acquisition time used in this study with the samples employed.

Proton reference spectra were acquired with the transmitter power attenuated by 10 dB relative to the 90° pulse transmitter power specified above at a receiver gain setting of 0-2 dB. Long-range ^1H-^{15}N heteronuclear shift correlation spectra were acquired using a receiver gain setting ranging from 16-20 dB, which did not lead to a receiver overload condition.

The long-range ^1H-^{15}N heteronuclear shift correlation experiments described in this work were performed using samples containing 15 mg of strychnine (0.045 mmole), 22 mg of brucine (0.055 mmole), or 12 mg of holstiine (0.03 mmole), each dissolved in 650 µl 99.96% d_6-DMSO (Cambridge Isotope Laboratories) or 99.96% deuteriochloroform (MSD Isotopes) as noted in the text.

REFERENCES AND NOTES

[1] R. C. Crouch and G. E. Martin, *J. Heterocyclic Chem.*, **32**, 1665 (1995).

[2] W. J. Chazin, L. D. Colebrok, and J. T. Edward, *Can. J. Chem.*, **61**, 1749 (1982).

[3] J. C. Carter, G. W. Luther III, and T. C. Long, *J. Magn. Reson.*, **15**, 122 (1974).

[4] D. A. Craig and G. E. Martin, *J. Nat. Prod.*, **49**, 456 (1986).

[5] A. L. Waterhouse, *Magn. Reson. Chem.*, **27**, 37 (1989).

[6] M. A. Bernstein and L. D. Hall, *Can. J. Chem.*, **63**, 483 (1985).

[7] A. Cherif, G. E. Martin, L. R. Soltero, and G. Massiot, *J. Nat. Prod.*, **53**, 793 (1990).

[8] R. C. Crouch, A. O. Davis, and G. E. Martin, *Magn. Reson. Chem.*, **33**, in press (1995).

[9] T. A. Carpenter, L. D. Colebrook, L. D. Hall, and G. K. Pierens, *Magn. Reson. Chem.*, **30**, 768 (1992).

[10] R. E. Hurd and B. K. John, *J. Magn. Reson.*, **91**, 648 (1991).

[11] J. Ruiz-Cabello, G. W. Vuister, C. T. W. Moonen, P. van Geldern, J. S. Cohen and P. C. M. van Zilj, *J. Magn. Reson.*, **100**, 282 (1992).

[12] R. C. Crouch and G. E. Martin, unpublished data.

[13] G. C. Levy and R. L. Lichter, Nitrogen-15 Nuclear Magnetic Resonance Spectroscopy, Wiley-Interscience, NY, 1979, p 11, pp 114-116.

[14] M. Witanowski, L. Stefaniak, and G. A. Webb, Nitrogen NMR Spectroscopy, Annual Reports in NMR Spectroscopy, G. A. Webb, ed, Vol **11b**, Academic Press, NY, 1981, pp 114-115.

[15] M. Witanowski, L. Stefaniak, and G. A. Webb, Nitrogen NMR Spectroscopy, Annual Reports in NMR Spectroscopy, G. A. Webb, ed, Vol **18**, Academic Press, NY, 1986, p 193.

[16] M. Witanowski, L. Stefaniak, and G. A. Webb, Nitrogen NMR Spectroscopy, Annual Reports in NMR Spectroscopy, G. A. Webb, ed, Vol **25**, Academic Press, NY, 1993, p 72.

[17] See ref. 14 pp 115-117, and references cited therein.

[18] G. E. Martin, R. C. Crouch, A. N. Tackie, M. J. M. Sharaf, and P. L. Schiff, Jr., to be published.

[19] C. W. Andrews, J. Wisowaty, A. O. Davis, R. C. Crouch, and G. E. Martin, *J. Heterocyclic Chem.*, **32**, 1011 (1995).

[20] G. E. Martin, R. C. Crouch, M. H. M. Sharaf, and P. L. Schiff, Jr., ^1H-^{15}N Direct and Long-Range Heteronuclear Shift Correlation Techniques — Potential Applications, 34th Annual Meeting of the American Society of Pharmacognosy, San Diego, CA, July, 1993, Poster 101.

[21] MacroModel V4.5; F. Mohamadi, N. G. J. Richards, W. C. Guida, R. Liskamp, C. Caufield, G. Chang, T. Hendrickson, and W. C. Still, *J. Comput. Chem.*, **11**, 440 (1990).

[22] N. L. Allinger, Y. H. Yuh, and J.-H. Lii, *J. Am. Chem. Soc.*, **111**, 8551 (1989); *ibid.*, **111**, 8566 (1989); *ibid.*, **111**, 8576 (1989); and subsequent MM3 references.

[23] R. C. Crouch, A. O. Davis, T. D. Spitzer, G. E. Martin, M. H. M. Sharaf, P. L. Schiff, Jr., C. H. Phoebe, Jr., and A. N. Tackie, *J. Heterocyclic Chem.*, **32**, 1077 (1995).